2025年臺灣國際科學展覽會 優勝作品專輯

作品編號 090026

參展科別 醫學與健康科學

作品名稱 Trojan Horses in the Fight against Skin

Cancer

得獎獎項 三等獎

就讀學校 Gymnasium Kirchenfeld

指導教師 Gobran Sarah

作者姓名 Xeno Messmer

作者照片



Abstract

In photodynamic therapy (PDT), reactive oxygen species are generated within the cytoplasm to destroy cancer cells selectively. Using porphyrinic structures (PS) as photosensitizers holds promise for targeting cancer cells. However, direct incorporation of the porphyrins into cancer cells remains elusive. Hence, *Dr. Martina Vermathen's* research introduced specific membranous phospholipid nanocarriers for topical porphyrin applications. However, since a sufficiently high enough concentration of PS in cancer cells has not yet been achieved, this study aimed to improve skin uptake of the nanocarriers.

Two approaches were examined: (1) comparing polar and nonpolar porphyrins and (2) assessing the effect of a penetration enhancer, DMSO, through a neat and diluted application.

The polarity of the porphyrins was first quantified with a log P test. The nanocarriers were assembled by incorporating two different PS compounds, either the mono- or tetra-4-carboxy substituted phenyl porphyrin. They were then characterized by 1D and 2D-NMR analysis. The porphyrin permeation was tested by Franz diffusion tests on pig ear skin. For the second approach, DMSO was added in the Franz diffusion test, either directly applied on the skin ("neat") or diluted in the nanocarriers ("diluted").

The log P test for the mono- and the tetra-carboxyphenyl porphyrin resulted in values of 4.5 and -1.1, respectively. The more polar tetra-carboxyphenyl porphyrin exhibited 2.8 times better skin uptake compared to the mono-carboxyphenyl porphyrin. The neat DMSO application increased uptake by a factor of 5.5. The diluted DMSO application worsened skin uptake slightly. Analytical techniques revealed differences in porphyrin encapsulation: The mono-carboxyphenyl porphyrins were encapsulated in the centre, whereas tetra-carboxyphenyl porphyrins were localised around the nanocarriers.

Results indicated potential instability of the nanocarriers. The more polar tetra-substituted porphyrins showed superior skin diffusion than the mono-substituted derivative. The neat DMSO application facilitated enhanced skin uptake by inducing membrane destabilization and pore formation but may have limited applicability.

Further research is suggested to explore porphyrinic PS with alternative polar substitution patterns and tailored penetration enhancers for lipid-based delivery systems. Overall, the study underscores the importance of molecular properties of the PS system and demonstrates the potential of penetration enhancers in optimizing PDT for skin cancer treatment.

TABLE OF CONTENTS

1. Introduction	1
1.1 Aim of this Work	2
1.3 Test Set-up	3
2. Materials and Methods	4
2.1 Materials	4
2.2 Methods 2.2.1 PBS Buffer Solution 2.2.2 Assembly of the Bicelles 2.2.3 Modified Assembly of the Bicelles 2.2.4 NMR Spectroscopy 2.2.5 Pig Ear Skin 2.2.5 Franz Diffusion Test on Pig Ear Skin 2.2.6 Modified Franz Diffusion Test on Pig Ear Skin 2.2.7 UV-Vis / Fluorescence Spectroscopy 2.1.8 Log P Test	5 5 5 6 6 7 8 9 9
3. Results and Discussion	10
3.1 Hydrophilic Properties 3.2.1 ¹ H-NMR 3.2.2 ¹ H- ¹ H NOESY 2.2.3 ¹ H DOSY	10 11 12 14
3.3 Skin Uptake	16
 3.4 Mono vs. Tetra 3.5 Penetration Enhancer 3.5.1 Encapsulation of the Diluted Approach 3.5.2 Skin Uptake with DMSO 3.6 Diluted with DMSO vs. Neat 	18 19 19 20 22
4. Conclusion and Outlook	24
6. Appendix	24
List of Figures	28
References	29
Decleration of Independence	30

1. Introduction

Photodynamic therapy (PDT) is a promising approach to treat cancer in a more selective way compared to chemotherapy. The basic idea of PDT is to selectively activate toxic properties in the cancer cell without affecting healthy tissue [i]. The potential of PDT has been known since 1900, when Oscar Raab, a German medical student, discovered that microorganisms incubated with certain dyes, are killed in the presence of light but not in the dark [ii]. In the process of PDT, free radicals and singlet oxygen species are generated inside the cancer cells. To do so, a photosensitizing molecule (PS) is delivered to the cancer cell, where it is activated with light of a certain wavelength in the visible spectrum of 400-800 nm. This activation leads to an energy transfer from the PS to free oxygen in the cytoplasm resulting in free radicals and reactive singlet oxygen species, finally leading to an internal destruction of the cancer cell [iii]. In PDT, porphyrins have proved to be a highly effective PS, due to their tumor-selective and phototoxic properties and their quality to absorb light - near infrared (NIR) wavelengths between 600-900 nm, which are able to penetrate the skin deeper compared to shorter wavelengths [iv]. Today, starting from the 1970s, only five photosensitizers have been clinically approved. Of these 5 only one was approved for topical use, namely the porphyrin precursor 5-aminolevulinic acid (5-ALA) [v]. 5-ALA is administered via the skin, reaches the cancer cells and accumulates in the mitochondria. Once there, the phototoxic protoporphyrin IX (PpIX) is then synthesized from 5-ALA in the Heme reaction [vi], as seen in figure 1.

Figure 1. In mitochondria, the phototoxic protoporphyrin IX (right) is synthesized from 5-aminolevulinic acid (left).

The pathway *via* a precursor is needed, as a direct integration of the large porphyrin molecules into the cell is hindered by the skin [vii]. Even though the first successful *in vivo* test

with 5-ALA against pancreas cancer was performed in 1994, the mechanism of tumor destruction is not yet fully understood [viii].

The creation of singlet oxygen and free radicals is directly linked to the abundance of PS in the cell [ix]. Consequently, the goal of most studies is to increase the concentration of PS in cancer cells. A possible way to achieve that, is to deliver the PS directly into the cells [x]. However, this method brings along several difficulties. The planar conjugation of a porphyrin, which is needed for light absorption, leads in most cases to molecules which are highly hydrophobic and aggregate in aqueous solutions [xi]. However, for the PS to get absorbed by the skin and cross the cellular membrane, it must be slightly hydrophilic-amphiphilic [xii]. This contrast leads to the problem of poor cellular uptake and therefore a decrease in PDT effectiveness [xiii]. Efforts have been made to overcome this obstacle. The research group of Dr. Vermathen managed to build bicelles in which the PS can be encapsulated. These bicelles are obtained by the thorough mixing of long-chain and short-chain phospholipids in water, which then may take the form of membranous discs of 10-50 nm. They are phospholipid assemblies with closed lipid monolayers with a fatty acid core and a polar surface with properties similar to micelles, enabling them to potentially carry the PS through the skin and into the cell by fusing with the cellular membrane (figure 2). These constructs, consisting of the PS surrounded by bicelles are so-called nanocarrier systems [xiv].

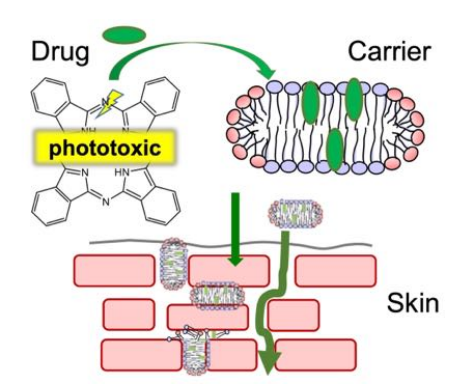


Figure 2. Simplified process of the nanocarriers delivering the PS to the skin cells [xv].

1.1 Aim of this Work

The aim of this work was to further improve uptake of the nanocarrier systems by the skin for the goal of achieving a sufficiently high enough concentration of PS in the cancer cells of epidermal non-melanoma topical skin cancer treatments such as Squamous Cell Carcinoma (SCC). To do so, two questions were investigated. First, if different substitution patterns of the porphyrin scaffold would affect encapsulation into the phospholipid carriers and

the skin penetration. Since to date, mostly nonpolar porphyrin PSs have been used. Secondly, it was tested if a penetration enhancer already in use in other formulas would work for nanocarriers by increasing their skin uptake.

1.3 Test Set-up

When attempting to increase the abundance of PS in skin cancer cells, the skin is the most important barrier to overcome for nanocarriers. In this regard, two different approaches were attempted towards an increase in skin uptake of the nanocarriers. In *approach 1*, the impact of substitution patterns, which lead to different polarities of the molecules, was investigated regarding bicelle encapsulation and skin uptake. To do so, two PDT-suitable porphyrins with different substitution patterns and therefore different polarities were compared. First, a porphyrin with one carboxyl group, namely 5-(4-Carboxyphenyl)-10, 15, 20-(triphenyl) porphyrin (1). The second molecule which was investigated is a porphyrin with four carboxyl groups, 5, 10, 15, 20-(Tetra-4-carboxyphenyl) porphyrin (2). Both are displayed in *figure 4*. These porphyrins will be referred to as the *mono-*(1) and *tetra-*(2) substituted porphyrin.

$$CO_2H$$
 NH
 NH
 NH
 CO_2H
 CO_2H
 NH
 NH
 NH
 CO_2H
 CO_2H

Figure 3. The unsymmetrical nonpolar *mono*-substituted porphyrin on the left, the symmetrical polar *tetra*-substituted porphyrin on the right.

In approach 2, it was tested whether penetration enhancers already in use in other formulas would work for nanocarrier systems by increasing their skin uptake. Two ways how a penetration enhancer could be deployed were tested with the *tetra*-substituted porphyrin. A diluted way and a neat way. For the diluted way, it was attempted to encapsulate the penetration enhancer into the bicelles and for the neat way, the penetration enhancer was applied directly onto the skin beforehand. Dimethyl sulfoxide (DMSO) was chosen as the penetration enhancer since it is already established and easy to obtain [xvi]. DMSO is well established for topical pharmaceutical applications, but controversial due to its side effects. It is FDA-approved to treat one condition, namely interstitial cystitis. REACH and ECHA classified no

hazards whereas CLP notifications identifies this substance as causing serious eye irritation, skin irritation and may cause respiratory irritation. DMSO disrupts lipid organisation and may displace protein-bound water. This is largely due to its amphiphilic nature, where DMSO interacts with lipids at the stratum corneum, altering the structure of the peptide, which then changes the partition coefficient and therefore increases the permeability of molecules [xvii].

2. Materials and Methods

2.1 Materials

5-(4-Carboxyphenyl)-10, 15, 20-(triphenyl)porphyrin (s) (1)	≤100%	Porphychem
5, 10, 15, 20-(Tetra-4-carboxyphenyl)porphyrin (s) (2)	≤100%	Porphychem
1,2-Dihexanoyl- sn -Glycero-3-Phosphocholine (s) (DHPC) (3)	≥99%	Anatrace
1,2-Dimyristoyl-sn-Glycero-3-Phosphocholine (s) (DMPC) (4)	≥99%	Anatrace
Dimethyl sulfoxide (l)	≥99.5%	Carl Roth GmbH+Co. Kg
Methanol (l)	≥99.8%	Fisher Scientific
Chloroform (l)	≥99.9%	Biosolve Chimie
Disodium hydrogen phosphate (s)	≥99.5%	Hänseler AG
Potassium dihydrogen phosphate (s)	≥99.5%	Dr. Grogg Chemie AG
Sodium chloride (s)	≥99.8%	Schweizer Salinen AG
1-Octanol (l)	≥99%	Sigma Aldrich
Polyoxyethylene(80)sorbitan monolaurate (1) (Tween 80)	=98%	Anatrace
Frozen pig ear skin		Wüthrich Metzg AG

2.2 Methods

Following, the methods used for the experiments are described.

2.2.1 PBS Buffer Solution

All experiments were conducted with a non-deuterated and a deuterated phosphate-buffered saline solution. For the PBS buffer, three solutions were prepared. First, a NaCl stock solution, a 50 mM KH₂PO₄ solution and a 50 mM Na₂HPO₄ solution. *Stock solution:* 50 g of H₂O/D₂O and 0.9% NaCl (0,45 g) were mixed and vortexed, in a 50 ml flask at room temperature, until dissolved. *KH*₂*PO4 solution A:* KH₂PO₄ (0.15014 g) was mixed with 22 mL of the stock solution and vortexed in a 50 mL flask at room temperature, until dissolved. *Na*₂*HPO*₄ *solution B:* At room temperature, in a 50 mL flask Na₂*HPO*₄ (0.1958 g) was mixed with 22 mL of the stock solution. Next, 14 mL of solution A and 20 mL of solution B were mixed. Using a pH electrode, either more of the acid solution A or the basic solution B was added to adjust to a pH of 7.3.

This process was performed two times, once with distilled water for approximately 40 mL of final yield, and once with deuterated water for approximately 10 ml of final yield for NMR usages.

2.2.2 Assembly of the Bicelles

The nanocarriers had to be built first. Therefore, a 66 mM DHPC and a 33 mM DMPC with 5 mM porphyrin solution were prepared. *DHPC solution:* DHPC C-6 phospholipids (3, 0.053 g, 0.119 mmol, 1 eq.) were dissolved in 1.8 mL of the PBS buffer solution with deuterated water *(comp. 2.1.1)*, at room temperature in a 5 mL one-necked round-bottom flask. The resulting mixture was vortexed and sonicated before the flask was sealed and set aside for 24 h at room temperature, to obtain a completely dissolved solution.

DMPC solution: DMPC C-14 phospholipids (4, 0.040 g, 0.0594 mmol, 0.5 eq.) and porphyrin (1, 2, 0.075 eq.) were dissolved in methanol (900 μL) and chloroform (900 μL), at room temperature in a 5 mL one-necked round-bottom flask. The resulting mixture was vortexed and sonicated until the suspension was completely dissolved. This process should force the porphyrin molecules to get embedded into the DMPC phospholipid chains via non-covalent bonds [xviii].

Next, at room temperature, the solvent of the DMPC solution was evaporated *in vacuo* (44 °C, 30 mbar), before the DHPC solution was added. Due to the absence of porphyrin signals

with a different diffusion coefficient on the DOSY spectrum of the mono- and tetra-substituted porphyrin respectively (*figure 12,13*), it can be assumed, that approximately all of the 0.009 mmol porphyrin molecules have been successfully encapsulated into the bicelles, resulting in a yield near 100%.

The resulting mixture was vortexed and sonicated. When the residue was completely dissolved, the resulting mixture was cooled down to -78 °C (acetone dry-ice bath) for 1 min followed by heating to 50 °C (warm water bath) for 4 min. This cooling and heating process was repeated eight times while vigorously vortexed between cycles, resulting in the desired blackish product that was stored in a light-protected area. This freezing/heating process, which is called freeze/thaw cycles, is performed to force the bicelles to condense as much as possible, which enhances skin uptake [xix].

According to the procedure described above, 3 bicelle solutions were prepared. First, one with the *mono*-substituted porphyrin (1, 0.0059 g, 0.009 mmol, 0.075 eq.) second, one with the *tetra*-substituted porphyrin (2, 0.0071 g, 0.009 mmol, 0.075 eq.) and third, one with only DHPC-DMPC as a reference.

2.2.3 Modified Assembly of the Bicelles

For the first experiment with a penetration enhancer, the diluted way, a modified bicelle solution was needed. This modified solution would, if successful, have encapsulated DMSO molecules in the bicelles. Therefore, before the freeze/thaw cycles, DMSO was added in 60 w/w-% of the DMPC/DMPC material (34 µl) to the DMPC film at the same time as the DHPC solution was added. The mixture was then sonicated and vortexed and the freeze/thaw cycles were performed the same way as in section 2.2.2. This concentration of DMSO is the threshold where DMSO unfolds its effects on the skin in other encapsulated drug formulas [xx]. For the second experiment with a penetration enhancer, the neat way, a normal bicelle solution with the tetra-substituted porphyrin was used as described in section 2.2.6.

2.2.4 NMR Spectroscopy

All measurements were made with a 500 MHz Bruker NMR spectrometer and processed with 4.1.4 Topspin. For the porphyrins a ¹H spectrum was made and for the bicelles a ¹H, ¹H-¹H NOESY and a ¹H DOSY were needed to gain a profound structural understanding of the bicelles and their encapsulated porphyrins.

¹H NMR: ¹H NMR Spectroscopy works due to the principle of nuclei having a spin and being electrically charged. By applying a strong magnetic field, an energy transfer to the nuclei is

possible. This energy transfer is in the range of radio frequencies and is specific to the element and isotopes of that element. When a nucleus is excited, it jumps from base energy level to a higher energy level, after a short period of time the nuclei relax and fall back into their original base energy level. In this relaxation period, the energy is emitted with the same frequency and leads to a signal [xxi]. Since every nucleus has a specific resonance frequency, this can be exploited and used to gain a structural understanding of the molecules in your measured sample.

¹H-¹H NOESY: *Nuclear Overhauser Effect Spectroscopy* (NOESY) works by the principle of polarization. It shows the transfer of polarization between two nuclei when they are close together. This transfer happens through space rather than chemical bonds. It is distance dependent, which means we can see signals of nuclei that are closer than 5 Ångström. This distance is equivalent to about 4 times a H-H bond length [xxii]. The utilization of NOESY allows us to see if molecules are coupled even when they do not have covalent bonds, resulting in the cross peaks present on the spectra.

¹H DOSY: *Diffusion-ordered Spectroscopy* (DOSY) seeks to differentiate signals of nuclei according to their diffusion coefficient. It works on the principle of the *Brownian* self-diffusion of molecules. After an initial radiofrequency field pulse, two opposite gradient pulses of magnetization are applied along the long sample axis in the test tube, creating planes with different resonance frequencies. In between these two pulses, the molecules can diffuse away from their original area, resulting in a loss of intensity. If the molecules were of low molecular weight, many will have diffused away between pulses and the resulting intensity will be significantly lower. However, if the molecules were of high molecular weight, few would have diffused away, and the total emissions of the molecules are similar to the emissions after the first pulse [xxiii]. This difference can be exploited to understand if there are molecules in the test tube which differ in size and weight and therefore bear a different diffusion coefficient. Consequently, the location of the signals on the DOSY spectrum depends on the diffusion coefficient of the molecule, with small molecules bearing a high diffusion coefficient appearing further down and large molecules with a low diffusion coefficient further up on the spectrum.

2.2.5 Pig Ear Skin

Porcine ears were obtained from Wüthrich Metzg AG a butcher located in Münchenbuchsee, Switzerland. All ears originated from roughly 6-month-old pigs at the time of slaughter. Immediately following slaughter, the ears were severed and promptly frozen at -20 °C. To prepare skin samples for the Franz Diffusion test, the ears were thawed in a refrigerator, cleansed under cold tap water, and tried with a soft tissue. Next, the bristles were removed with an electrical trimmer. Using a sharp scalpel, the skin was separated from the cartilage starting from the cut at the base of the ear. Solely the skin on the dorsal side of the ears was used. As the skin was completely removed, it was cut into approximately 2 cm squares, wrapped in aluminum foil, and stored at -20 °C until the *Franz* diffusion tests.

2.2.5 Franz Diffusion Test on Pig Ear Skin

A *Franz* diffusion cell apparatus and the pig ear skin were used to recreate the conditions on the living tissue for the bicelles. To do so, a receptor medium for the receptor chamber was prepared. Non-deuterated PBS buffer *(comp. 2.1.1)* was mixed with 0.1% Tween 80, shaken and then sonicated for 30 min. To run the experiment as a triplicate, 3 pieces of about 2 cm² pig ear skin were thawed in the PBS buffer with non-deuterated water for about 30 min. They were then clamped under the donor chamber of the *Franz* diffusion cells *(figure 3)* with the outer skin side pointing upwards. The receptor chambers of the *Franz* diffusion cells were then filled up with receptor medium so that no air would remain in the chamber. A magnetic stirrer was added to each cell, the water pump was turned on, set to 32 °C and left to preheat for 30 min. After that, 500 μL of the bicelle-porphyrin solution (1) or (2) was added into all 3 donor chambers and the test was left running for 24 h.

Next, the remaining bicelle-porphyrin solution was removed with an *Eppendorf* pipette. The skin samples were then carefully removed from the donor chamber, thoroughly rinsed with distilled water and then brushed with distilled water, common soap and a cotton bud. Next, the 3 skin samples were submerged in a 62 °C hot water bath for 2.5 min to facilitate separating the epidermis from the dermis with a razor blade afterwards. Dermis and epidermis were cut into small pieces and added to separate flasks with DMSO (2 mL). The flasks were then sonicated for 20 min and set aside for 24 h in a dark place to let the porphyrins get extracted out of the skin. The resulting DMSO solutions were then examined by analytical measurement (UV-Vis and fluorescence spectroscopy) to calculate the amount of porphyrin molecules that passed the skin barrier and accumulated in the epidermis/dermis per square centimeter. For reference purposes, the receptor medium was also analyzed by UV-Vis and fluorescence spectroscopy to determine if some of the porphyrin solution passed through the whole membrane.



Figure 4. Franz diffusion apparatus with 3 cells (left), breakdown of a single cell (right) [xxiv].

2.2.6 Modified Franz Diffusion Test on Pig Ear Skin

For the second experiment with a penetration enhancer, the neat way, modified pig ear skins were needed. To do so, after the skin samples were thawed and clamped under the donor chambers, they were carefully dried with a tissue. Next, 500 µL of DMSO was added into the donor chamber of the cells onto the skins. After 15 min the solvent was removed with an *Eppendorf* pipette. The skins were once again dried up carefully with a tissue and the porphyrin bicelle solution could be added. The experiment was then performed the same way as described in section 2.2.5 but as a duplicate due to cost constraints.

2.2.7 UV-Vis / Fluorescence Spectroscopy

UV-Vis and fluorescence spectroscopy were used to determine the intensity of porphyrin fluorescence in the solutions of the dermis, epidermis, the receptor medium and the log P test. The intensities of the dermis and epidermis after the *Franz* diffusion test were then quantified with a calibration trendline by measuring multiple concentrations, which were plotted at peak intensity. With the help of the trendline the obtained fluorescence intensities of the dermis and epidermis could be quantified to concentrations (appendix 1, 2).

2.1.8 Log P Test

A log P test using the shake flask method had to be performed to quantify the polarity of the two different porphyrins. For this reason, a phase equilibrium and a porphyrin dilution had to be made first. *Phase equilibrium:* 5 ml n-octanol and 5 ml PBS buffer with non-deuterated water solution (comp. 2.1.1) were added into a sealable test tube. The tube was put into a mechanical shaker and left at max efficacy for 22 h until the two phases were completely separated. *Porphyrin dilution:* At room temperature, a 5 mM porphyrin (1, 2, 0.01 mmol) in 2 ml of DMSO solution was mixed, sonicated and vortexed well until the porphyrin was completely dissolved.

500 μL of the porphyrin solution was then added to the phase equilibrium with an *Eppendorf* pipette. The resulting mixture was put into the mechanical shaker at max capacity and left running for 22 h. Next, the test tubes were put into a centrifuge for 5 min to separate the phases completely. 2 mL of the n-octanol phase and 2 mL of the buffer phase were drawn up with a syringe and put in separate flasks. The two porphyrin solutions of the two phases were then characterized with UV-Vis and fluorescence spectroscopy. This process was performed for both the *mono*-substituted porphyrin (1, 0.0065 g) and the *tetra*-substituted porphyrin (2, 0.0079 g).

The log P values were then calculated using the peak intensity at a certain wavelength (*mono*-substituted 650 nm, *tetra*-substituted 652 nm). A log P value of 1 would mean that the compound has a 10:1 higher affinity to the lipid phase and one of -1 would mean the opposite.

3. Results and Discussion

3.1 Hydrophilic Properties

The log P test for the *mono*- and the *tetra*-substituted porphyrin resulted in a log P value of 4.5 and -1.1, respectively. This indicates that the *mono*-substituted porphyrin partitions itself to the lipid phase rather than the aqueous phase with a factor of 31623:1. This proves, that the unsymmetrical nonpolar molecule is very hydrophobic. In contrast, the symmetrical *tetra*-substituted porphyrin partitions better to the water phase than to the lipid phase with a factor of 1:13. Consequently, the polar *tetra*-substituted porphyrin has a more hydrophilic character, as seen in *figure 5*.



Figure 5. Log P test with the *mono*-substituted porphyrin (left) and the *tetra*-substituted porphyrin (right), at the top is the n-octanol phase and at the bottom the water pha

3.2 Encapsulation

3.2.1 ¹H-NMR

In *figure 6*, the ¹H-NMR spectrum (*comp. 2.2.4*) of the bicelle solution with the *mono*-substituted porphyrin assembled as described in section *2.2.2*, the characteristic signals of the bicelles between 0.5-5.5 ppm (*appendix 3*) and the characteristic *mono*-substituted porphyrin signals between 7.8-8.9 ppm (*appendix 1*) can be observed. Based on this result, it can be assumed that the *mono*-substituted porphyrin molecules were at least partly encapsulated into the bicelles. If the porphyrin molecules did not encapsulate into the bicelles and were just in the solution, they would have aggregated in the aqueous mixture, and it would not be possible to observe the porphyrin signals using this measurement method.

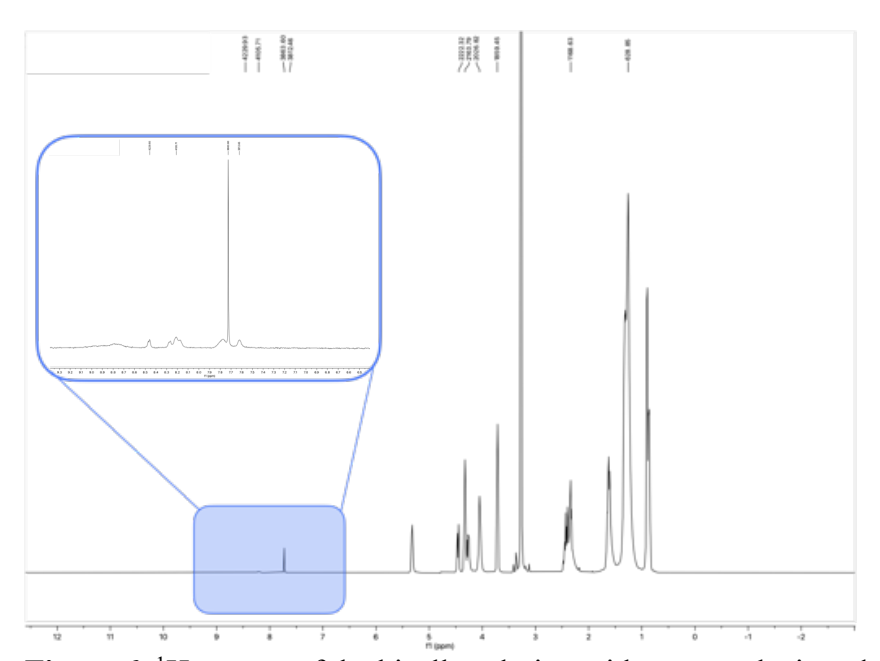


Figure 6. ¹H spectra of the bicelle solution with *mono*-substituted porphyrin.

In *figure* 7, the ¹H spectrum (*comp.* 2.2.4) of the bicelle solution with the *tetra*-substituted porphyrin assembled as described in section 2.2.2, the characteristic signals of the *tetra*-substituted porphyrins (*appendix* 2) can be seen between 7.5-9 ppm. This indicates that part of the porphyrin molecules have successfully been integrated.

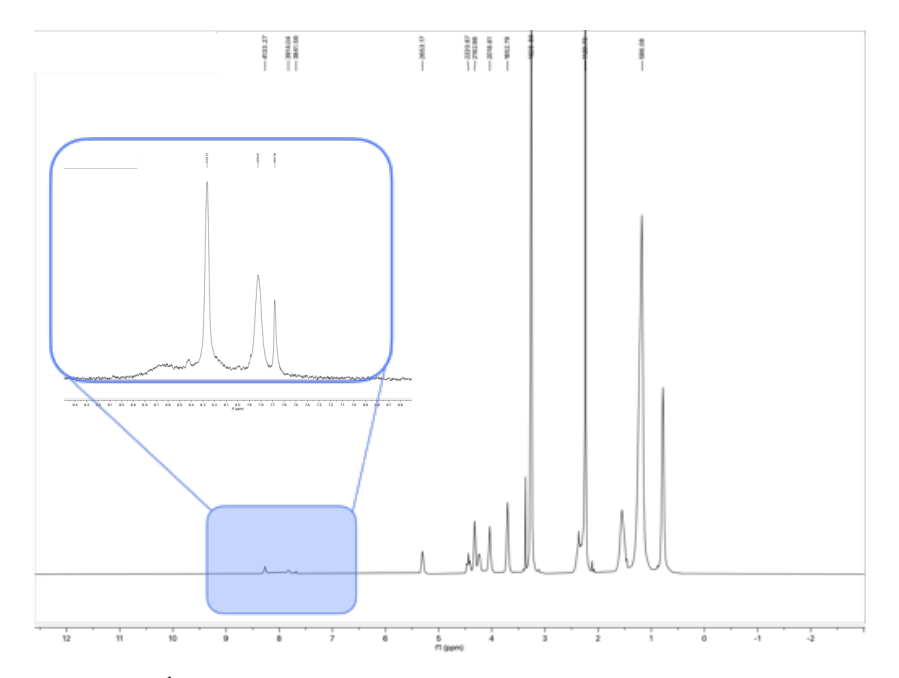


Figure 7. ¹H-NMR spectrum of the bicelle solution with the tetra-substituted porphyrin.

Based on the results of the ¹H-NMR spectra, no comparison can yet be drawn between the encapsulation of the *mono*-substituted and the *tetra*-substituted porphyrin. However, it can be qualitatively stated that the encapsulation worked for both porphyrins. Only if the encapsulated porphyrins were represented in a quantitative amount, a ¹H-NMR spectrum of such a high peak resolution can be obtained. Therefore, a considerable amount of both porphyrins has successfully been encapsulated into the bicelles.

3.2.2 ¹H-¹H NOESY

The 2D ¹H-¹H NOESY spectrum (*comp. 2.2.4*) of the bicelle solution with the *mono*-substituted porphyrin assembled as described in section 2.2.2, shows the cross peaks that indicate the interactions of the phospholipids and the porphyrins with themselves (*figure 8*). This was expected since both porphyrin and liposome protons show intramolecular interactions. However, the peaks in region "a" (*figure 8*) indicate that the porphyrins also interacted with the phospholipids. More precisely, they interacted exclusively with the CH₃ groups of the tail regions of the phospholipids. These intermolecular interactions show that the porphyrins have successfully been encapsulated and are located deep within the bicelles (*figure 9*).

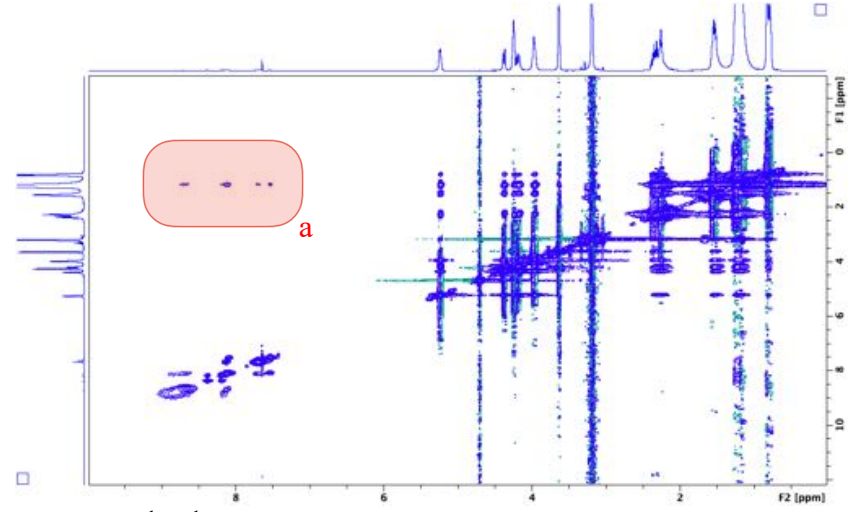


Figure 8. ¹H-¹H NOESY spectrum of the bicelle solution with the *mono*-substituted porphyrin.

Figure 9. DMPC liposome, CH₃ groups where the porphyrin molecules are located at are marked in red.

On the NOESY spectrum (comp. 2.2.4) of the tetra-substituted porphyrin bicelle solution assembled as described in section 2.2.2, the intramolecular interactions/cross peaks of the porphyrins and the liposomes are also visible (figure 10). In region "a" we can see that the tetra-substituted molecules have encapsulated themselves successfully as well. In contrast to the mono-substituted porphyrin however, there are interacting signals from the CH₃ tail regions up to the ammonium head regions of the phospholipids. This means that the porphyrin molecules are located all around on the inside of the bicelles (figure 11). Hence, it can be assumed that some molecules even stick on the outside of the bicelles, possibly making them structurally unstable.

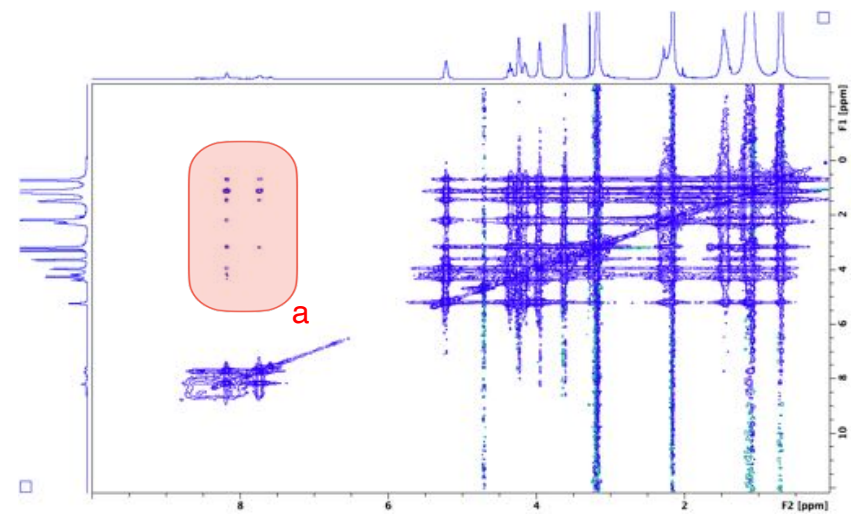


Figure 10. ¹H-¹H NOESY spectrum of the bicelle solution with the *tetra*-substituted porphyrin.

Figure 11. DMPC liposome, CH₃ groups where the porphyrins are located are marked in red.

By comparing these two NOESY spectra, the first difference regarding encapsulation becomes apparent. The porphyrin molecules that were encapsulated gathered at very different locations in the bicelle. Whilst the *mono*-substituted porphyrin stayed deep in the center of the bicelles (figure 9), the tetra-substituted porphyrin was all around the phospholipids (figure 11). This difference can be explained by the obtained log P values of both porphyrins. The more hydrophobic *mono*-substituted porphyrin (log P 4.51) avoided the hydrophilic head region and gathered at the also hydrophobic tail regions of the lipids. On the other hand, the more hydrophilic tetra-substituted porphyrin (log P -1.1), gathered itself all around the phospholipid molecule.

2.2.3 ¹H DOSY

On this spectrum (figure 12), the bicelle solution with the mono-substituted porphyrin assembled as described in section 2.2.2, was analyzed with diffusion ordered spectroscopy (comp. 2.2.4). All peaks in figure 12 are located at the same height, which indicates that in the solution only one kind of particle is present. Hence, it can be assumed that the porphyrins have been integrated into the bicelles. Furthermore, the lack of peaks of non-encapsulated porphyrins with a higher diffusion coefficient proves that of the 5 mM porphyrin given to the bicelles, every porphyrin molecule has successfully been encapsulated.

Moreover, in region "a" one can see a zig-zag line present in the range of 0.5-1.5 ppm where the signals of the CH₂ and the CH₃ groups appear *(appendix 3)*. This zig-zag line on the spectrum indicates that the small DHPC lipids are prone to split away from the longer DMPC chains, which leads to an opening of the bicelles. DHPC and DMPC molecules have different diffusion coefficients as long as they are not bonded together. Therefore, this action of separation leads to the zig-zag line. Thereby, it must be assumed that the bicelles were not entirely structurally stable products after they were constructed.

The signals which appear in region "b" are most likely caused by residual CHCl₃ in the solution and are not further discussed here.

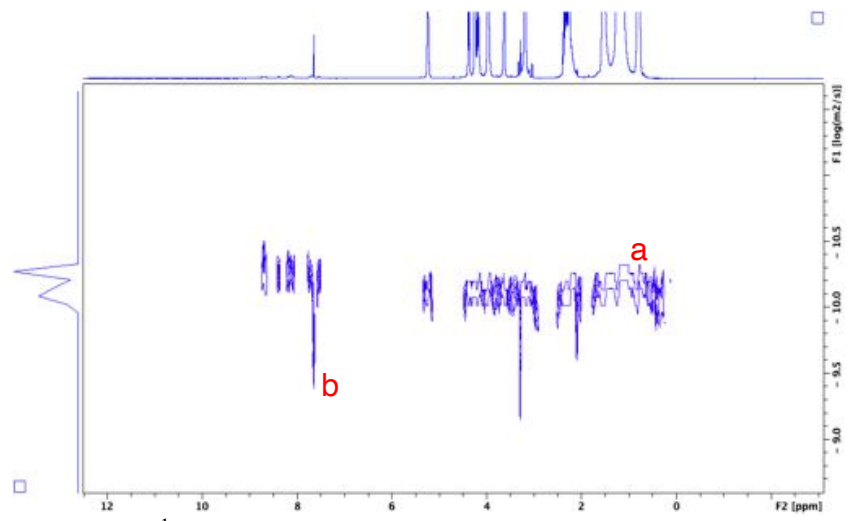


Figure 12. ¹H DOSY spectrum of the bicelle solution with the *mono*-substituted porphyrin.

On the DOSY spectrum (comp 2.2.4) of the tetra-substituted porphyrin bicelle solution assembled as described in section 2.2.2, all signals are in line with the assumption that all present molecules have the same diffusion coefficient (figure 13). This indicates that all porphyrin molecules are successfully encapsulated. Furthermore, in region "a" the zig-zag line is again present, hinting at unstable bicelles. In region "b" a descending signal can be observed. This is caused by the residual peak of methanol which overlaps with the peak of the lipids, resulting in a signal that "smears out" downwards.

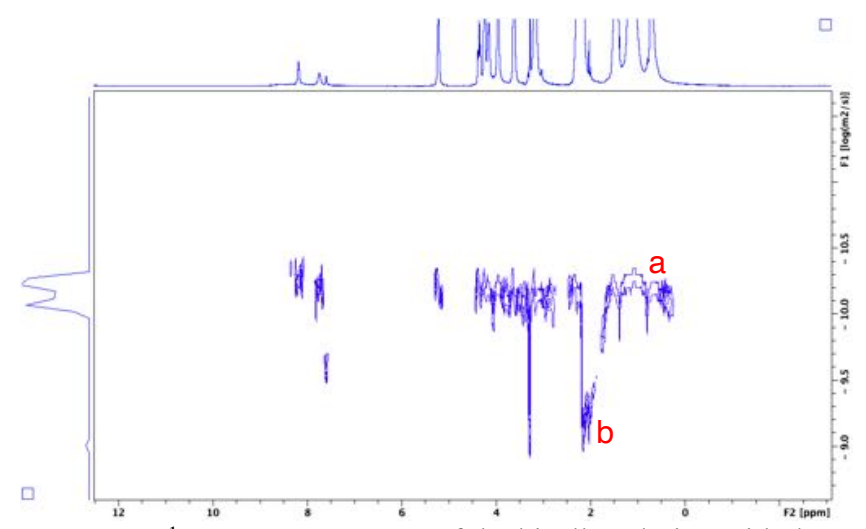


Figure 13. ¹H DOSY Spectrum of the bicelle solution with the *tetra*-substituted porphyrin.

By drawing the comparison between these two DOSY spectra, it can be stated that both *mono*-substituted and *tetra*-substituted porphyrin were entirely encapsulated into the nanocarrier system. There are indications for a destabilizing effect which occurs since DHPC seems to exit from the bicelle assembly and is in exchange with the water phase. This may lead to a disintegration of the bicelles when in touch with the skin in the *Franz* diffusion test. This may also be of advantage because a part of the DHPC might act as a penetration enhancer itself. However, it is not possible to draw a conclusion about if the *mono*-substituted or the *tetra*-substituted porphyrin-bicelle nanocarrier system penetrates the skin better, from just the NMR data.

3.3 Skin Uptake

On this diagram (figure 14) we can see the results of the Franz diffusion test, as described in section 2.2.2. It displays the amount of mono-substituted porphyrin (1) molecules in nanograms, which successfully crossed the skin barrier into the epidermis or the dermis per square centimetre. Cells 1-3 represent the sample size. From the results, three outcomes become evident. First, a considerable amount of porphyrin molecules penetrated the skin from the 500 µl starting material applied on the skin, which consisted of 1646875 ng mono-substituted porphyrin. Second, that experiments with real skin are prone to get different results, therefore triplicates were made. Third, that many of the bicelles penetrated the skin deeply and released their porphyrin molecules into the dermis skin layer.

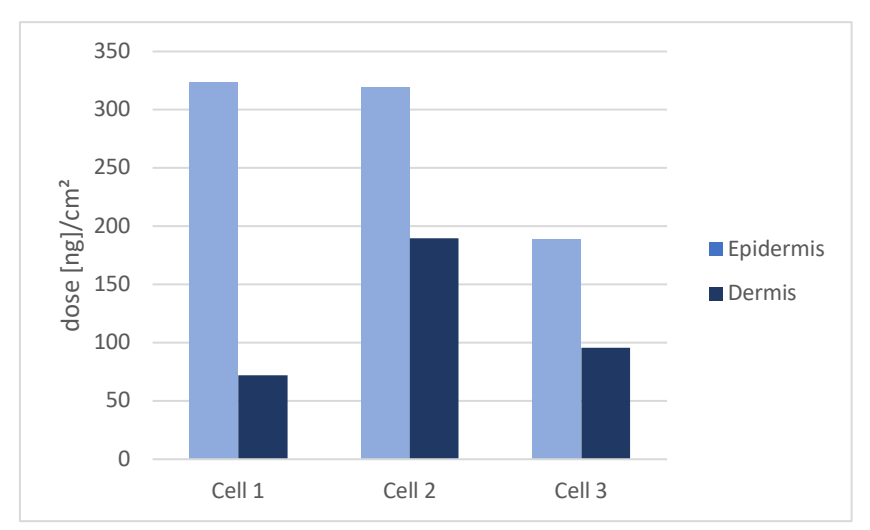


Figure 14. Franz diffusion results with the mono-substituted porphyrin, Exp. 1.

The three results of the *tetra*-substituted porphyrin (2) experiment, as described in section 2.2.2, proved to be more similar (*figure 15*). Again, a considerable amount of porphyrin molecules penetrated the skin from the 500 µl starting material applied on skin, which consisted of 1976900 ng *tetra*-substituted porphyrin molecules. The lack of the dermis bar in cell 1 is caused by a cut in the dermis of the sample skin, which led to an unusable result. Additionally, analytical measurements of the receptor fluid have shown that only a negligible amount of porphyrins have been found in the receptor fluid of both applications (not shown).

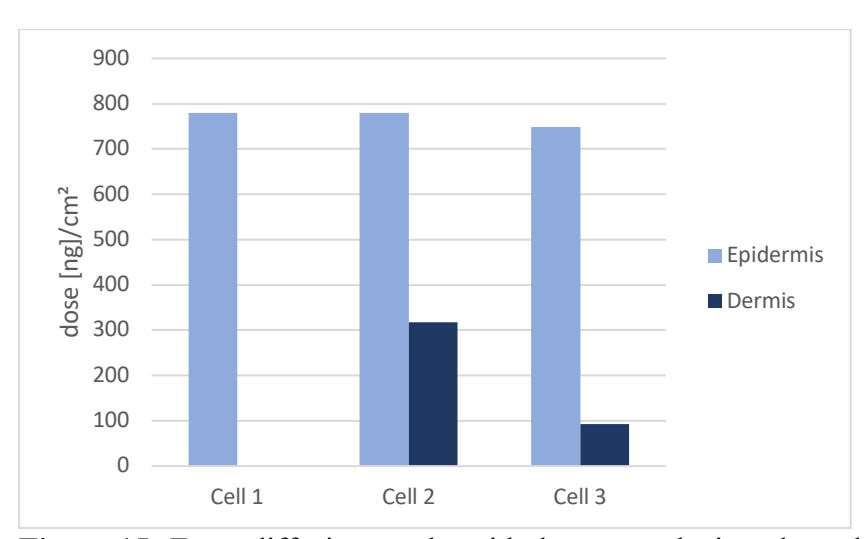


Figure 15. Franz diffusion results with the tetra-substituted porphyrin, Exp. 2.

By taking the average amount of the two *Franz* diffusion experiments, a more precise comparison between the two porphyrins (*figure 16*) can be made. Surprisingly, the *tetra*-substituted porphyrin portrayed a better uptake than the *mono*-substituted porphyrin. Whereas on

average 769.0 ng/cm² of the *tetra*-substituted porphyrin, only 277.2 ng/cm² of the *mono*-substituted porphyrin crossed the skin barrier into the epidermis. This correlates to a factor of 2.8. Within the dermis the difference is not that significant, scoring 205.3 ng/cm² for the *tetra*-substituted and 119.2 ng/cm² for the *mono*-substituted porphyrin. Furthermore, the ratio between epidermis and dermis is at 3.7 for the *tetra*-substituted and at 2.3 for the *mono*-substituted porphyrin. This indicates that although the *mono*-substituted bicelles spiked with porphyrin molecules crossed the skin barrier less effectively, they penetrated more deeply into the dermis. However, both did not pass the whole membrane.

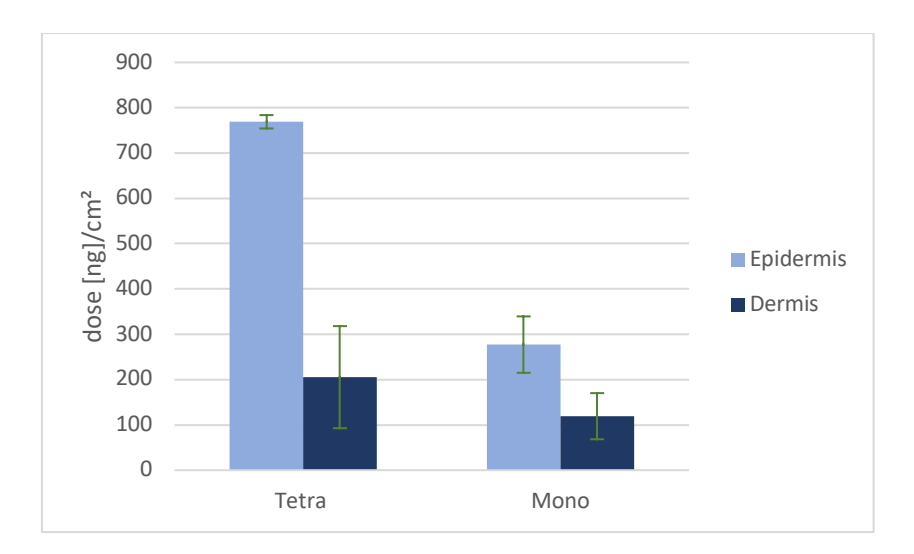


Figure 16. Comparison of the skin uptake of the two porphyrins, Exp. 1 and 2.

3.4 Mono vs. Tetra

The results of the *Franz* diffusion test prove that contrary to initial assumptions, the hydrophilic polar *tetra*-substituted porphyrin outperformed the hydrophobic nonpolar *mono*-substituted porphyrin PS by a large margin, by a factor of 2.8. There are several possible explanations for this phenomenon. First, it is possible that the extremely hydrophobic *mono*-substituted porphyrins started to aggregate right when the bicelles fused with the cellular membranes. If this happened, the *mono*-substituted porphyrins would suddenly be released into a very different, aqueous environment resulting in aggregating and in the loss of their PDT ability and consequently becoming undetectable to the fluorescence spectrometer. This would mean one would only see the remaining porphyrins which did not get released into the cells, hence, explaining the unexpected results. There are however limitations to these results. Mainly, the purity of the encapsulation of the porphyrins into the bicelles was tested indirectly via ¹H-DOSY. For these experiments to work there must be an equal yield of *mono* and *tetra*-porphyrin encapsulated into the bicelles. However, it can be assumed that the yield

of both porphyrins was the same, but this can be further validated by NMR concentration experiments in the future. For reference purposes, empty bicelles were also analysed with the same NMR methods and can be found in appendix 3.

Second, it became apparent that the more outside localisation of the tetra-substituted porphyrin on the bicelles promoted its diffusion into the skin. The effect might be beneficial for skin uptake. It could have resulted in the porphyrins leaving the bicelles more easily and consequently resulting in more *tetra*-substituted porphyrin molecules leaving the bicelles in the skin medium. This is backed by the fact that the presumably more stable bicelle and porphyrin construct of the *mono*-substituted were prone to penetrate deeper into the dermis rather than accumulating in the epidermis. That being said, for both porphyrins only a negligible amount of porphyrins have been found in the receptor medium, indicating that both did not penetrate through both epidermis and dermis. Nonetheless, the deeper penetration of the *mono*-substituted porphyrin is not favorable for epidermal non-melanoma skin cancer treatments such as Squamous Cell Carcinoma (SCC), as the cancer cells are located in the upper skin layers and the treatment intends to be defined at a specific location, rather than being spread by reaching the hypodermis. Since the skin uptake of the tetra-substituted porphyrin worked better, it was chosen for the further experiments with the penetration enhancer DMSO.

3.5 Penetration Enhancer

3.5.1 Encapsulation of the Diluted Approach

On this DOSY spectrum (comp. 2.2.4) we can see the signals of the modified bicelle solution, where it was attempted to encapsulate DMSO into the bicelles (comp. 2.2.3), depicted in figure 17. Whilst ¹H and the ¹H-¹H NOESY NMR characterization has not shown any differences between the normal tetra-substituted porphyrin spectra and the spectra of tetra-substituted porphyrin with encapsulated DMSO, the ¹H DOSY spectrum (figure 17) shows in region "a" the characteristic solvent peak of DMSO-d6 at 2.5 ppm. Because of the lower weight of the molecule, the signal has a larger diffusion coefficient but due to the U-shaped signal it can be assumed that, if at all, only some of the DMSO molecules may be encapsulated into the lipids, possibly disrupting the structure of the bicelles. This is backed up by the fact that the bicelles without encapsulated DMSO and Photosensitizer do not show such a U-Shaped signal (appendix 3). The in figure 17 depicted regions "b" and "c" are artefacts of the spectrum and are hence not important for this discussion.

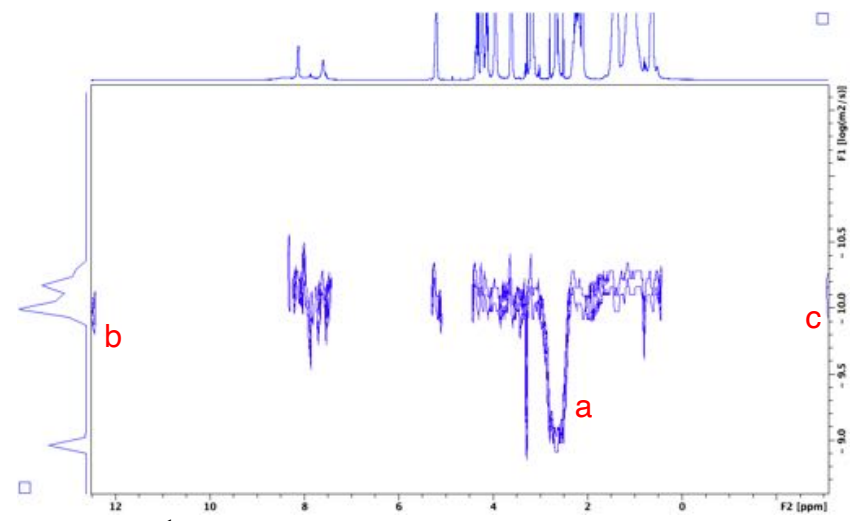


Figure 17. ¹H DOSY Spectrum of the bicelle solution with the *tetra*-substituted porphyrin with 60 w/w-% DMSO.

3.5.2 Skin Uptake with DMSO

On this diagram (*figure 18*) are the results of the *Franz* diffusion test presented which was performed with a modified *tetra*-substituted porphyrin bicelle solution containing 60 w/w-% of the hopefully encapsulated penetration enhancer DMSO, as described in section 2.2.3. The diluted way. Due to time and money constraints a 2-cell experiment was made.

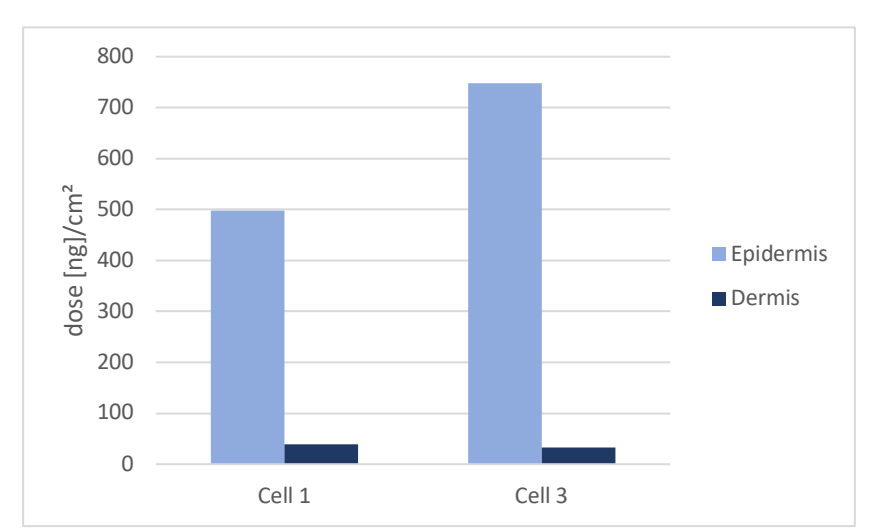


Figure 18. *Franz* diffusion results of the *tetra*-substituted porphyrin with encapsulated DMSO, Exp. 3.

Figure 19 shows the results for the Franz diffusion test with the penetration enhancer DMSO used to prepare the skin before the experiment (comp. 2.2.6). 2 ml/cm² of DMSO was applied to the skin for 15 minutes before the bicelle solution was added. The neat way. Again a 2-cell experiment was made.

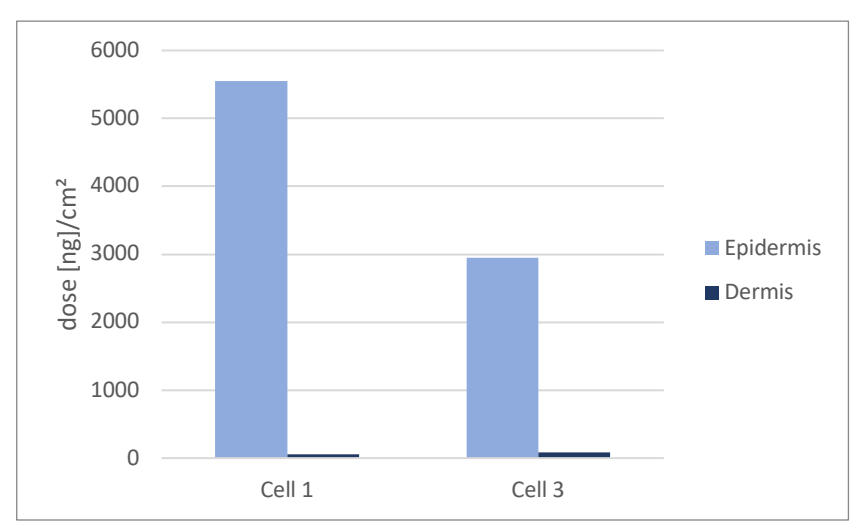


Figure 19. *Franz* diffusion results of the *tetra*-substituted porphyrin with DMSO applied to the skin, Exp. 4.

Using the average of the 2 cell experiments a quantitative comparison between the different ways can be made (*figure 20*). First, it can be seen that the encapsulated DMSO did not enhance skin uptake. As 622.7 ng/cm² with encapsulated DMSO stand against 769 ng/cm² for the normal *tetra*-substituted skin uptake. From these results it can be assumed that encapsulated DMSO may even decrease skin uptake. However, this assumption is vague since the standard deviation in these *Franz* diffusion tests is large. The encapsulated DMSO did however improve the ratio between epidermis and dermis, increasing it from 3.7 to 17.5. In conclusion, the DMSO in the mixture may have decreased skin uptake but prevented the bicelles from reaching deep into the dermis.

The second way proved to be more successful. 4254.1 ng/cm² of porphyrin in bicelles crossed the skin barrier contrary to 769 ng/cm² which crossed the skin barrier without the DMSO treatment. This is an improvement of a factor of 5.5. Also, the ratio of epidermis/dermis with DMSO applied to the skin is 62.5 compared to the standard ratio of 3.7 without the usage of a penetration enhancer. Therefore, the applied DMSO not only increased uptake significantly, but also led to the porphyrin molecules accumulating more in the epidermis rather than in the dermis, which is favorable.

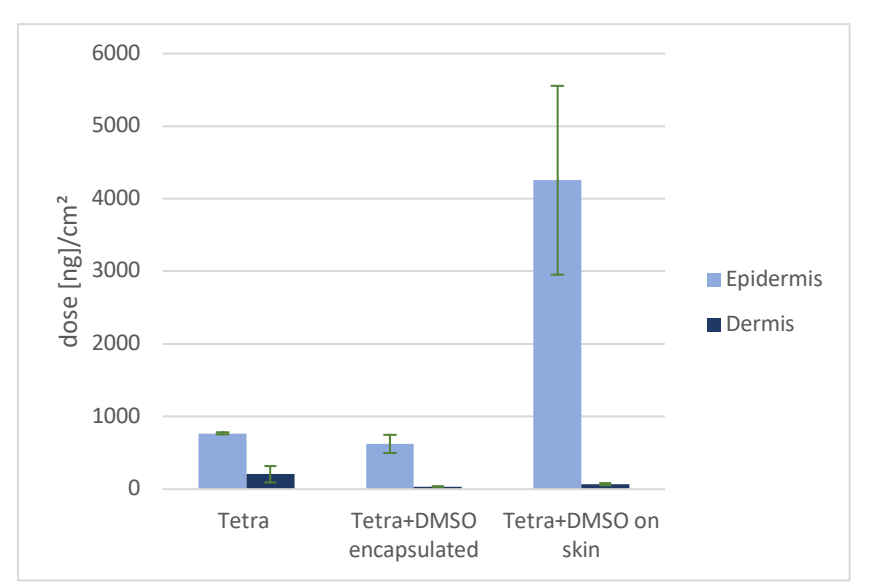


Figure 20. Comparison between the normal *tetra*-substituted porphyrin and the two employments of DMSO, Exp. 2, 3, 4.

3.6 Diluted with DMSO vs. Neat

The application of dimethyl sulfoxide (DMSO) as a penetration enhancer proved to be very successful if used with the right approach. From the Franz diffusion results, we see that the neat approach worked extraordinarily well, boosting skin uptake by a factor of 5.5, but the diluted approach may even worsen skin uptake. It can be assumed that this difference probably originates from the mechanism of how DMSO acts as a penetration enhancer on the skin. It is not yet understood how DMSO inflicts its enhancing properties, especially for hydrophilic molecules. However, there is evidence that two major events occur when DMSO is applied to human skin. Firstly, the DMSO molecules gather just below the head group regions of the skin membrane lipid bilayers. By doing so, the molecules act as spacers between the lipids and cause a less dense and more permeable packing arrangement of the stratum corneum [xxv]. It alters the structure of the peptide, the membrane becomes "floppy". This changes the partition coefficient and therefore increases the permeability of molecules. Secondly, at high concentrations, the DMSO molecules can even encourage/induce and stabilize water pore formation. A spontaneous reaction occurs when two lipids on opposite sides of each other sink into the membrane bilayer, forming a small opening in the membrane. This reaction can occur in normal membrane systems but is not stable enough to have a noticeable effect. If the reaction is now supported with DMSO molecules, the molecules enter the bilayer, position themselves under the head groups regions and consequently facilitate the entry of water molecules into the bilayer. This formation occurs until the lipids rearranged themselves into an hourglass shape, with a continuous flow of water rushing through the resulting

stable pore [xxvi]. This is a proposed theory of the King's College London which is backed by numerous simulations that are supported by experimental data shown in *figure 21*.

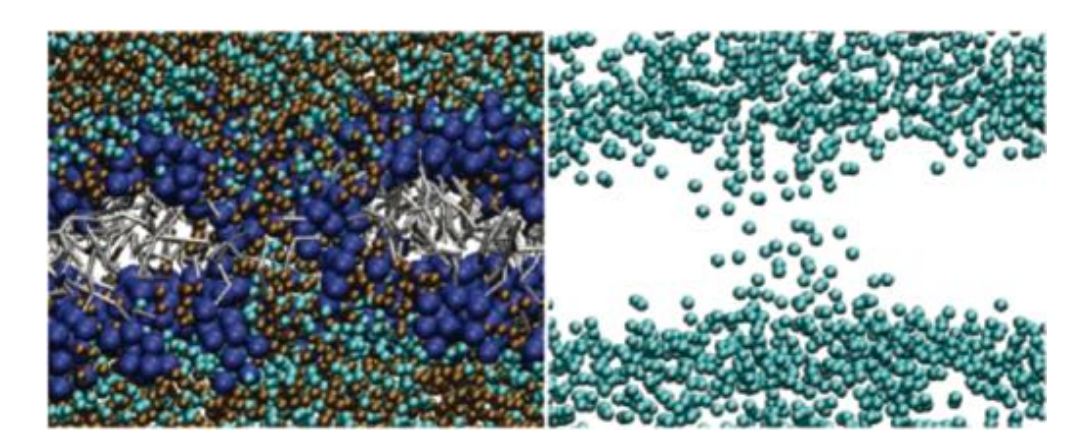


Figure 21. Water pore formation in a tensionless DPPC bilayer with 27 mol % DMSO after 261.4 ns. Water molecules are shown in cyan, DMSO in brown, DPPC headgroup and glycerol backbone particles in blue, and hydrocarbon particles in light gray (left). Just the water molecules shown in cyan (left) [xxvii].

These two possible mechanisms would explain the observed phenomenon of the experiments. Since on one hand, the less dense membrane and the induced water pores would explain why the *Franz* diffusion with a high concentration of DMSO on the skin was much more successful (Exp. 4). It can also be assumed that these mechanisms are the reason why experiment 3 with the diluted DMSO solution performed slightly worse than the normal *tetra*-substituted bicelle one (Exp. 2). If the DMSO, which was added to the bicelles, gathered under the head regions of the membrane bilayer of the bicelles, it would have made them less dense and therefore bigger in size. Since size is the determining factor for skin uptake, this would explain the worse results of experiment 3. This theory is backed up by the obtained NMR data (*figure 17*), where it could be seen that some DMSO molecules stuck to the bicelles. The direct employment of DMSO is therefore not helpful for nanocarrier systems built with phospholipids.

Contrary to common belief, large doses of DMSO over a prolonged time of exposure on the skin show only minor toxic effects like itching or burning. DMSO is approved by the FDA for one specific topical application, i.e. interstitial cystitis and has already numerous pharmaceutical formulas [xxviii]. This is why it could be used in future applications of topically applied nanocarriers, carrying photosensitizing molecules.

4. Conclusion and Outlook

Within the scope of this work, two main conclusions could be drawn. First, a comparison between polar porphyrin PSs and nonpolar porphyrin PSs could be made through numerous different results regarding their hydrophilic properties, their encapsulation into the bicelles and most importantly, their final skin uptake. It was shown that the *tetra*-substituted porphyrin had a better skin uptake by a factor of 2.8. Hence, it can now be qualitatively stated that porphyrinic PSs with polar substitution patterns should be favored in future studies about lipid-based delivery systems for topical applications of porphyrinic PSs. With further experiments, this result could be further validated. For example, by comparing other porphyrins with different functional groups such as OH groups, which again differ in polarity.

The second approach proved to be very successful. Evidence showed that the application of a penetration enhancer can enhance skin uptake of the nanocarriers by a factor of 5.5, if applied the right way. This is a promising result for future studies and the factor of 5.5 can be further optimized using different penetration enhancers already used in topically applied dosage forms. For example, penetration enhancers such as Azone® or propylene glycols. These penetration enhancers might be more tailored to increase skin uptake of nanocarriers and should thus be tested. However, with the promising results of the approach, it proves the potential of penetration enhancers for this application.

In the future these may have been modest but important contributions to the goal of developing a safe-to-use, topically applied nanocarrier PS formula, which can precisely and exclusively kill skin cancer cells.

6. Appendix

In this part of the thesis the conducted ¹H-NMR and fluorescence experiments are listed. The corresponding molecules are depicted above.

APPENDIX LIST

1. Analytical data of 1	25
2. Analytical data of 2	26
3. Analytical data of 3.4	27

1. Analytical data of *5-(4-Carboxyphenyl)-10, 15, 20-(triphenyl)porphyrin* (1) ¹H NMR (500 MHz, DMSO) δ 8.84, 8.37, 8.33, 8.22, 7.85, 3.33, 2.49, 1.24, 0.85, -2.92.

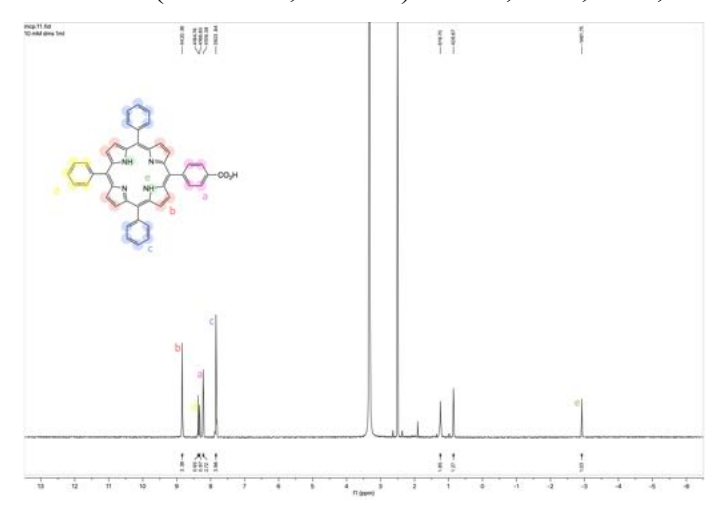


Figure 22. ¹H-NMR spectrum of (1).

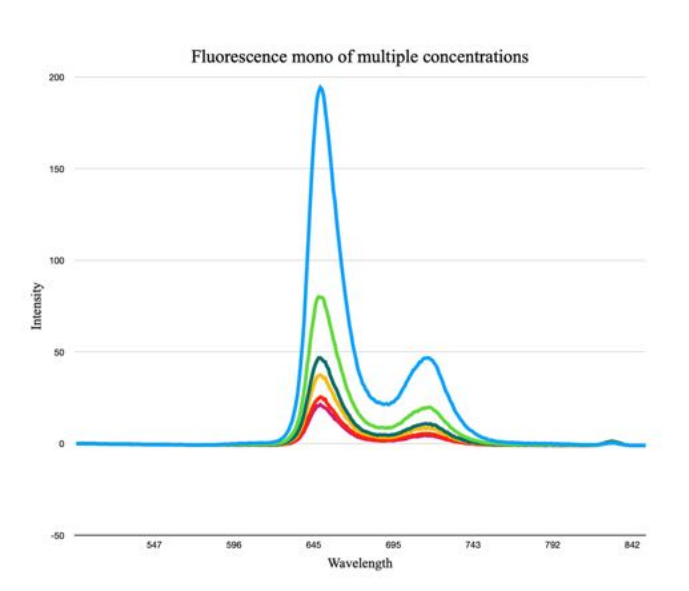


Figure 23. Fluorescence intensities of the mono-substituted porphyrin at multiple concentrations.

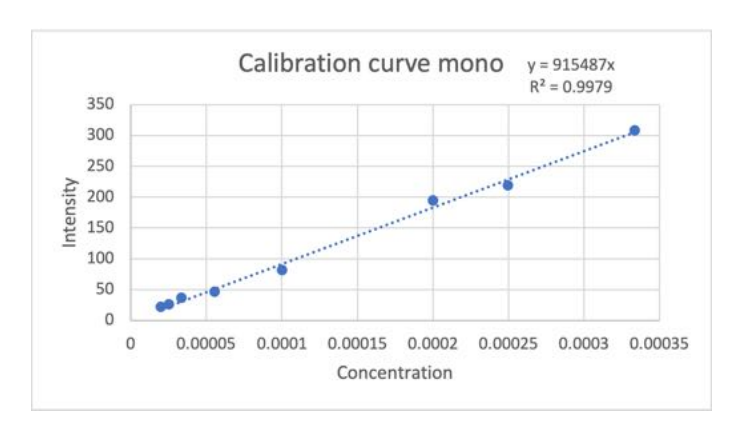


Figure 24. The mono-substituted subsequent calibration curve plotted at 650 nm

2. Analytical data of 5, 10, 15, 20-(Tetra-4-carboxyphenyl)porphyrin (2)

¹H NMR (500 MHz, DMSO) δ 13.28, 8.85, 8.37, 8.34, -2.94.

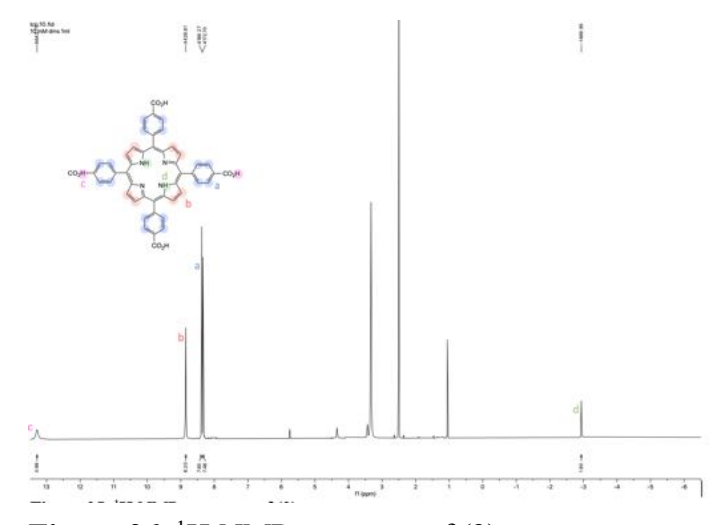


Figure 26. ¹H-NMR spectrum of (2).

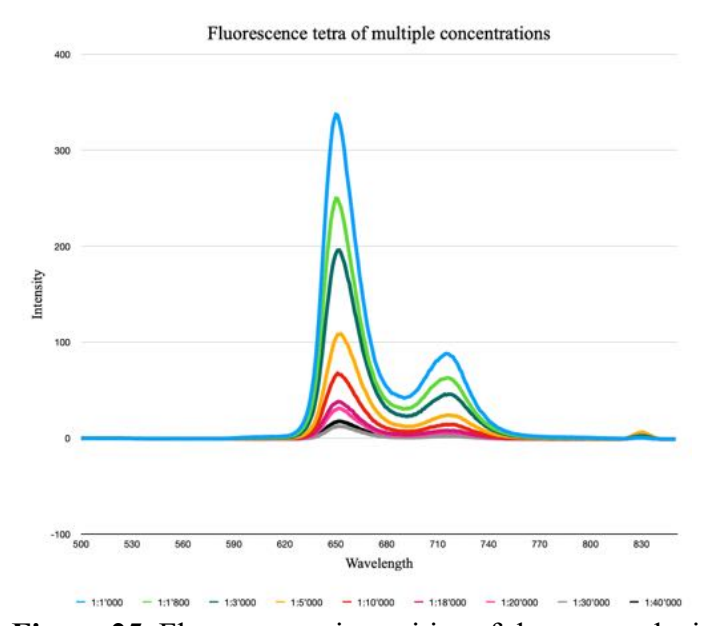


Figure 25. Fluorescence intensities of the *tetra*-substituted porphyrin at multiple concentrations.

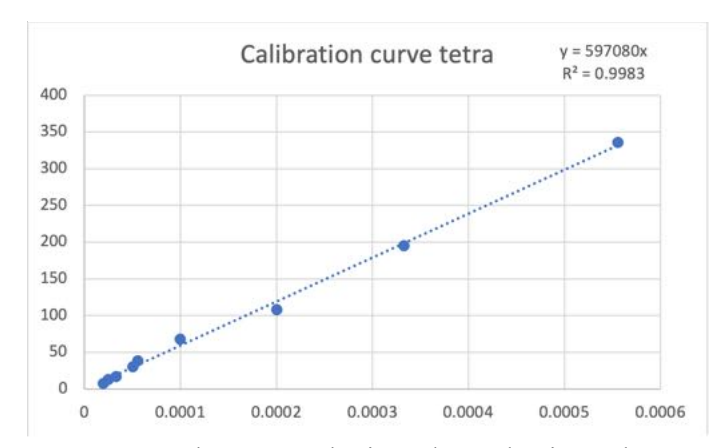


Figure 27. The tetra-substituted porphyrins subsequent calibration curve plotted at 652 nm.

3. Analytical data of 1,2-Dihexanoyl- *sn* -Glycero-3-Phosphocholine (*DHPC C-6*) **(3)**, 1,2-Dimyristoyl-*sn*-Glycero-3-Phosphocholine (*DMPC C-14*) **(4)**

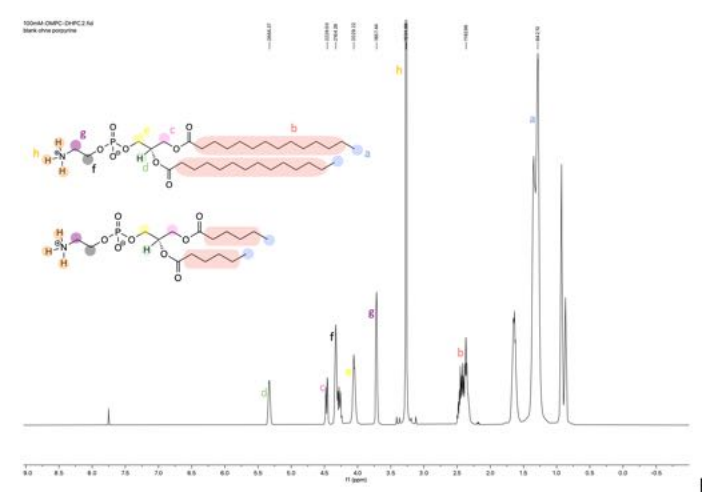


Figure 28. ¹H spectrum of (3), (4).

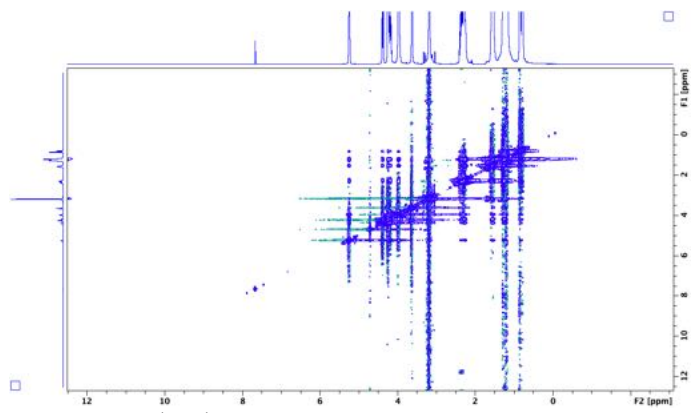


Figure 29. ¹H-¹H NOESY spectrum of (3), (4).

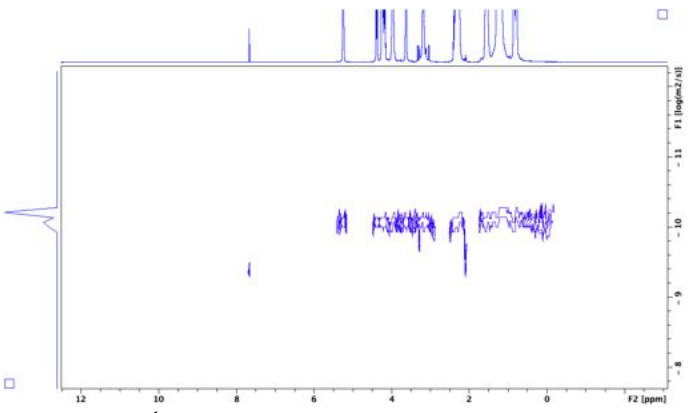


Figure 30. ¹H DOSY spectrum of (3), (4).

List of Figures

Figure 1. In mitochondria, the phototoxic protoporphyrin IX (right) is synthesized from 5- aminolevul	inic
acid (left).	1
Figure 2. Simplified process of the nanocarriers delivering the PS to the skin cells [xv]	2
Figure 3. The unsymmetrical nonpolar $mono$ -substituted porphyrin on the left, the symmetrical polar t	tetra-
substituted porphyrin on the right.	3
Figure 4. Franz diffusion apparatus with 3 cells (left), breakdown of a single cell (right) []	9
Figure 5. Log P test with the mono-substituted porphyrin (left) and the tetra-substituted porphyrin (rig	ght), at
the top is the n-octanol phase and at the bottom the water pha	10
Figure 6. ¹ H spectra of the bicelle solution with <i>mono</i> -substituted porphyrin.	11
Figure 7. ¹ H-NMR spectrum of the bicelle solution with the tetra-substituted porphyrin	12
Figure 8. ¹ H- ¹ H NOESY spectrum of the bicelle solution with the <i>mono</i> -substituted porphyrin	13
Figure 9. DMPC liposome, CH3 groups where the porphyrin molecules are located at are marked in re	ed 13
Figure 10. ¹ H- ¹ H NOESY spectrum of the bicelle solution with the <i>tetra</i> -substituted porphyrin	14
Figure 11. DMPC liposome, CH3 groups where the porphyrins are located are marked in red	14
Figure 12. ¹ H DOSY spectrum of the bicelle solution with the <i>mono</i> -substituted porphyrin	15
Figure 13. ¹ H DOSY Spectrum of the bicelle solution with the <i>tetra</i> -substituted porphyrin	16
Figure 14. Franz diffusion results with the mono-substituted porphyrin, Exp. 1	17
Figure 15. Franz diffusion results with the tetra-substituted porphyrin, Exp. 2.	17
Figure 16. Comparison of the skin uptake of the two porphyrins, Exp. 1 and 2	18
Figure 17. ¹ H DOSY Spectrum of the bicelle solution with the <i>tetra</i> -substituted porphyrin with 60 w/v	<i>N</i> −%
DMSO.	20
Figure 18. Franz diffusion results of the tetra-substituted porphyrin with encapsulated DMSO, Exp. 3	20
Figure 19. Franz diffusion results of the tetra-substituted porphyrin with DMSO applied to the skin, E	Exp. 4.
	21
Figure 20. Comparison between the normal <i>tetra</i> -substituted porphyrin and the two employments of D	OMSO,
Exp. 2, 3, 4.	22
Figure 21. Water pore formation in a tensionless DPPC bilayer with 27 mol % DMSO after 261.4 ns.	Water
molecules are shown in cyan, DMSO in brown, DPPC headgroup and glycerol backbone particle	es in
blue, and hydrocarbon particles in light gray (left). Just the water molecules shown in cyan (left)	[] 23
Figure 22. ¹ H-NMR spectrum of (1)	25
Figure 23. Fluorescence intensities of the mono-substituted porphyrin at multiple concentrations	25
Figure 24. The mono-substituted subsequent calibration curve plotted at 650 nm	25
Figure 25. ¹ H-NMR spectrum of (2)	26
Figure 26. Fluorescence intensities of the <i>tetra</i> -substituted porphyrin at multiple concentrations	26
Figure 27. The tetra-substituted porphyrins subsequent calibration curve plotted at 652 nm	26
Figure 28. ¹ H spectrum of (3), (4).	27
Figure 29. ¹ H- ¹ H NOESY spectrum of (3), (4)	27
Figure 30. ¹ H DOSY spectrum of (3), (4)	27

References

- [i] Hauner, K., Maisch, P. & Retz, M. (2017) Side effects of chemotherapy. *Urologe A*, **56**, 472-479.
- [ii] Kato, H. (1996) [History of photodynamic therapy--past, present and future]. *Gan To Kagaku Ryoho*, **23**, 8-15.
- [iii] Kwiatkowski, S. et al. (2018) Photodynamic therapy mechanisms, photosensitizers and combinations. *Biomed Pharmacother*, **106**, 1098-1107.
- [iv] Ash, C. et al. (2017) Effect of wavelength and beam width on penetration in light-tissue interaction using computational methods. *Lasers Med Sci*, **32**, 1909-1918.
- [v] Moan, J. & Peng, Q. (2003) An outline of the hundred-year history of PDT. *Anticancer Res*, **23**, 3591-3600.
- [vi] Wachowska, M. et al. (2011) Aminolevulinic Acid (ALA) as a Prodrug in Photodynamic Therapy of Cancer. *Molecules*, 16, 4140-4164.
- [vii] Sharadha, M. et al. (2020) An overview on topical drug delivery system Updated review. *International Journal of Research in Pharmaceutical Sciences*, **11**, 368-385.
- [viii] Juarranz, A. et al. (2008) Photodynamic therapy of cancer. Basic principles and applications. *Clin Transl Oncol*, **10**, 148-154.
- [ix] Sztandera, K., Gorzkiewicz, M. & Klajnert-Maculewicz, B. (2020) Nanocarriers in photodynamic therapy-in vitro and in vivo studies. *Wiley Interdiscip Rev Nanomed Nanobiotechnol*, **12**, e1509.
- [x] Sztandera, K., Gorzkiewicz, M. & Klajnert-Maculewicz, B. (2020) Nanocarriers in photodynamic therapy-in vitro and in vivo studies. *Wiley Interdiscip Rev Nanomed Nanobiotechnol*, **12**, e1509.
- [xi] Andrade, S.M. et al. (2008) Self-aggregation of free base porphyrins in aqueous solution and in DMPC vesicles. *Biophys Chem*, **133**, 1-10.
- [xii] Moret, F. & Reddi, E. (2017) Strategies for optimizing the delivery to tumors of macrocyclic photosensitizers used in photodynamic therapy (PDT). *Journal of Porphyrins and Phthalocyanines*, **21**, 239-256.
- [xiii] Lo, P.C. et al. (2020) The unique features and promises of phthalocyanines as advanced photosensitisers for photodynamic therapy of cancer. *Chem Soc Rev*, **49**, 1041-1056.
- [xiv] Sadasivam, M. et al. (2013) Self-assembled liposomal nanoparticles in photodynamic therapy. *European Journal of Nanomedicine*, **5**.
- [xv] Furrer, J. & Vermathen, M. (2022) Topical delivery systems for NIR absorbing Photosensitizers Designed for Dermal Application: Topics for Bachelor/Master Students in Chemistry [PDF]. University Bern.
- [xvi] Williams, A.C. & Barry, B.W. (2004) Penetration enhancers. Adv Drug Deliv Rev, 56, 603-618.
- [xvii] Marren, K. (2011) Dimethyl sulfoxide: an effective penetration enhancer for topical administration of NSAIDs. *Phys Sportsmed*, **39**, 75-82.
- [xviii] Gjuroski, I., Furrer, J. & Vermathen, M. (2021) Probing the Interactions of Porphyrins with Macromolecules Using NMR Spectroscopy Techniques. *Molecules*, **26**, 1942.
- [xix] Bos, J.D. & Meinardi, M.M. (2000) The 500 Dalton rule for the skin penetration of chemical compounds and drugs. *Exp Dermatol*, **9**, 165-169.

- [xx] Notman, R. et al. (2007) The permeability enhancing mechanism of DMSO in ceramide bilayers simulated by molecular dynamics. *Biophys J*, **93**, 2056-2068.
- [xxi] Singh, M.K. & Singh, A. (2022) Nuclear magnetic resonance spectroscopy. In *Characterization of Polymers and Fibres*, Elsevier, pp. 321-339.
- [xxii] Agarwal, N. et al. (2018) Characterization of Nanomaterials Using Nuclear Magnetic Resonance Spectroscopy. In *Characterization of Nanomaterials*, Elsevier, pp. 61-102.
- [xxiii] Gouilleux, B., Rouger, L. & Giraudeau, P. (2018) Ultrafast 2D NMR: Methods and Applications. In *Annual Reports on NMR Spectroscopy*, Elsevier, pp. 75-144.
- [xxiv] PermeGear, 2022. Franz Cell the original [Online]. PermeGear. Available from: https://permegear.com/franz-cells/ [Accessed October 2, 2023].
- [xxv] Capriotti, K. & Capriotti, J.A. (2012) Dimethyl sulfoxide: history, chemistry, and clinical utility in dermatology. *J Clin Aesthet Dermatol*, **5**, 24-26.
- [xxvi] Notman, R. et al. (2006) Molecular basis for dimethylsulfoxide (DMSO) action on lipid membranes. *J Am Chem Soc*, **128**, 13982-13983.
- [xxvii] Notman, R. et al. (2006) Molecular basis for dimethylsulfoxide (DMSO) action on lipid membranes. London: *J Am Chem Soc*, fig.
- [xxviii] Marren, K. (2011) Dimethyl sulfoxide: an effective penetration enhancer for topical administration of NSAIDs. *Phys Sportsmed*, **39**, 75-82.

Decleration of Independence

1. I hereby declare that I have created the present project of the National Contest for Swiss Youth in Science

Trojan Horses in the Fight against Skin Cancer

Testing different approaches for enhancing skin permeability

in topical applications of photodynamic therapy

independently and without unauthorized outside help and that all sources, resources and websites have been used truthfully and are documented

Zurich, 16. 11. 2024

AMM-

【評語】090026

1. Novelty and Significance:

This project addresses a critical challenge in photodynamic therapy (PDT) for cancer treatment: improving the skin uptake of porphyrinic photosensitizers. The research is significant as it explores innovative approaches to enhance PDT efficacy, potentially leading to more effective skin cancer treatments.

2. Strengths:

Comprehensive methodology, utilizing various analytical techniques such as log P tests, NMR analysis, and Franz diffusion tests.

Comparative analysis of different porphyrin structures and application methods, providing valuable insights for optimizing PDT delivery systems.

Investigation of both molecular properties (porphyrin polarity) and delivery methods (use of penetration enhancers), demonstrating a multi-faceted approach to the problem.

3. Weaknesses:

Lack of quantitative data on absolute porphyrin uptake, making it difficult to assess the clinical relevance of the findings.

Potential instability of nanocarriers, which could limit practical applications.

Absence of in vivo studies or photodynamic activity assessments, which would provide more comprehensive insights into the efficacy and safety of the proposed improvements.